Coherent pion effects at large rapidities in nucleus-nucleus collisions

G. Z. Obrant
Petersburg Nuclear Physics Institute, Leningrad Region, Gatchina 188350, Russia
(Received 6 March 1996)

Coherent effects are considered in the model of bremsstrahlung of scalar pions in high-energy nucleus-nucleus collisions. As a result of the quantum mechanical Monte Carlo calculation it is shown that this mechanism yields pions in central collisions at large rapidities with a strong coherence. The coherent enhancement of the cross section has a threshold character of a function of the number of interacting nucleon pairs. The coherence narrows regions of pion transverse momenta towards zero and longitudinal momenta around some characteristic value. The pion pseudorapidities are moved to large values of about one-half of a unit. [S0556-2813(96)02910-X]

PACS number(s): 25.75.Dw, 02.70.Lq, 13.75.Gx, 24.10.Lx

I. INTRODUCTION

The large pion multiplicity in the STAR project at RHIC ($\sim 10^3$) could allow the observation of a new physical phenomenon—the classical pion field, analogous to the laser electromagnetic field. Some experimental evidence of its existence comes from Centauros (anti-Centauros) events in cosmic ray physics with an anomalously small (large) number of π^0 [1,2]. Such isospin fluctuations were explained as pion identity effects in a model of pion coherent states [3] and in the case of multipion states with a strong coherence [4,5]. Analogous effects were obtained for the classical pion field in the nonlinear sigma model [6]. The creation of such a field for the nucleus-nucleus collision was studied in [7]. The production of the classical pion field is widely discussed now in connection with the idea of the disoriented chiral condensate (DCC) [8–25]. In this case the observation of pion coherent effects may be a signature of the vacuum phase transition.

Besides the isospin fluctuations an important feature of Centauros events is a large rapidity value of emitted hadrons, $\langle \eta^{\mathrm{lab}} \rangle = 9.9 \pm 0.2$ [2]. Assuming Centauros events to be generated at the energy $E \approx 1740$ TeV during the collision of the projectile nucleus $A=60$ with the target nucleus $A=14$ we obtain the energy $\sqrt{S_{NN}} \approx 234$ GeV and the rapidity $\langle y_{NN} \rangle = 9.9 - 5.5 = 4.4$ in the nucleon-nucleon c.m. system. These parameters correspond to the kinematics of future experiments at RHIC. The aim of this work is to study the influence of coherent effects connected with Bose enhancement factors due to pion symmetrization on the nucleus-nucleus collisions in the region of large rapidities.

One can understand the main features of the coherent pion production in the large rapidity region by virtue of a simple model of bremsstrahlung of scalar pions, only one pion being radiated in every elementary nucleon-nucleon interaction. The characteristic angles for such emission are $\theta \approx m/p$. Here p denotes the nucleon momentum and m is the nucleon mass. If there is a strong interference of pion waves from different sources in such scattering (that is not trivial because of large pion momenta), then two effects must take place. The first one is the narrowing of the transverse momenta region for pions (p_t distribution). This effect must occur when a few sources localized in the large transverse space region R radiate pion waves coherently. In this case the characteristic transverse momentum becomes $p_t \sim 1/R$ by virtue of the symmetrization on pions from different sources. It is significantly smaller than the inverse transverse space range for the elementary process.

The second effect is the analogous narrowing of the longitudinal momentum distribution due to pion coherence. It could take place if the longitudinal range in the pion momentum space for elementary pion creation does not exceed strongly the inverse longitudinal nucleus space range taking into account the Lorentz shortening. The narrowing of the distribution occurs around some value, being characteristic for the pion bremsstrahlung mechanism. As a consequence of the narrowing of the p_t spectrum and the fact that the coherence does not soften the longitudinal momenta the pseudorapidity distribution moves to the right. The narrowing of the longitudinal momentum distribution makes this effect more pronounced.

The value of the coherent effects discussed for the single-inclusive-pion distribution depends on two factors. The first one is the small probability for all N pions of a multipion system to be in the same quantum state. The second factor is the laser-type $N!$ enhancement of a cross section due to a coherence [4,5]. As a result, the coherent effects in the central nucleus-nucleus collisions demonstrate a drastic threshold character as a function of the number of interacting nucleon-nucleon pairs. The coherent effects could be large enough for observing them in the STAR project at RHIC.

In Sec. II the amplitude of the pion radiation in the nucleus-nucleus scattering is treated via some model of the pion bremsstrahlung. In Sec. III the quantum mechanical Monte Carlo method of amplitude and cross-section calculations is described. The results of calculations are discussed in Sec. IV for the simple deuteron-deuteron case and in Sec. V for gold nucleus collisions. The estimation of coherent effects in the case of the large number of pion sources is done in Sec. VI. Some remarks about the experimental observation of effects discussed is offered in Sec. VII although we are only at the beginning stage of an understanding of coherent phenomena. In the Appendix some details of the calculations are presented.

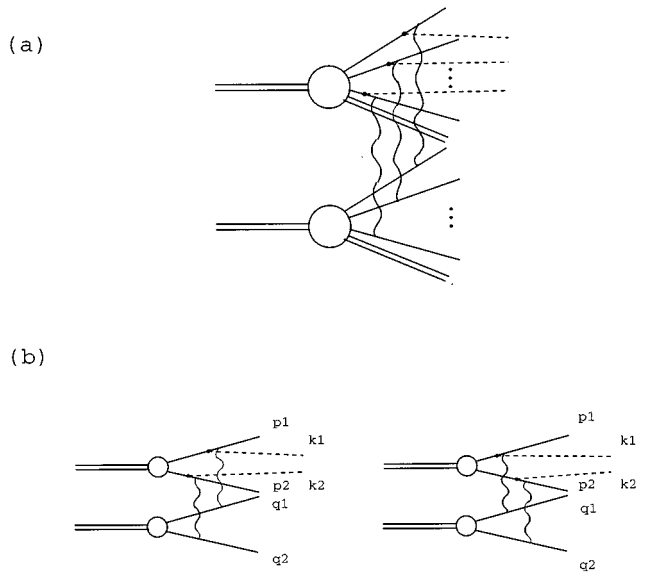

FIG. 1. The amplitudes of the pion radiation for the nucleus-nucleus collision in the general case (a) and in the deuteron-deuteron sample (b).

II. THE AMPLITUDE OF PION RADIATION

To study quantitatively coherent phenomena in nucleus-nucleus collisions some phenomenological model of the multiperipheral type could be chosen. To understand the main qualitative effects in this task we consider now the simple model of the bremsstrahlung of scalar pions. Besides for the simplicity it corresponds to the kinematics of pion creation, possessing the important property of the transverse momenta restriction. The central nucleus-nucleus collisions are studied with an energy of 100 GeV per nucleon in the c.m. system. The main question to be treated is the problem of pion coherence with the large number of pions. If the average multiplicity in the nucleon-nucleon scattering is $\langle n\rangle$ and the number of interacting nucleon-nucleon pairs is denoted by N, then we will consider collisions with multiplicity more than $\langle n\rangle N$. For central collisions N corresponds to the nucleus atomic weight. To understand qualitatively the main features of the collisions it is convenient for simplicity to study the model with $\langle n\rangle = 1$. Then one can consider only the diagrams with one pion radiation in every nucleon-nucleon interaction [Fig. 1(a)]. We will discuss the kinematical region of large pion longitudinal momenta and small transverse ones. Such diagrams may interfere strongly with pion permutations at such kinematics. We neglect amplitudes with radiation of pions from one nucleon line without radiation from another one. They cannot possess significant interference with the pion permutation in the case of large longitudinal pion momenta [26]. After such radiation the nucleons in the final state will have different longitudinal momenta (see Fig. 3 in Sec. IV) and the amplitude with the pion permutation will be small in this kinematical region. The situation is opposite to the case of soft gluon interference in QCD [27] where just such diagrams provide the strong coherent effects.

To understand all the peculiarities of the scattering mechanism it is convenient to begin from the deuteron-deuteron case as the simplest first step. A one-loop graph of the old perturbation theory, Fig. 1(b) presents the amplitude, Eq. (1), which is given by a threefold integral on the nucleon momentum in the intermediate state:

$$M=\int \frac{d^3p_1'}{(2\pi)^3}\,\frac{1}{2E(p_1')2E(p_2')2E(q_1')2E(q_2')} \times\frac{G(S_p)}{E_0-E(p_1')-E(p_2')}\,\frac{G(S_q)}{E_0-E(q_1')-E(q_2')} \times\frac{1}{E_1+i\eta-E(p_1')-E(q_1')}\,\frac{M_1}{h_1^2-m^2}\,\frac{M_2}{h_2^2-m^2}, \quad (1)$$

$$h_i^2=[E(p_i)+E(q_i)-E(q_i')]^2-(\mathbf{p}_i'-\mathbf{k}_i)^2 \quad (i=1,2).$$

The value E_0 is the initial deuteron energy, $E(p)$ and $\omega(k)$ are the nucleon and meson energies, and $E_1=E(p_1)+E(q_1)+\omega(k_1)$. The structure of Eq. (1) is transparent. The form factors $G(S_p)$ and $G(S_q)$ with the corresponding energy denominators represent the wave functions of rapidly moving deuterons. They are the infinite momentum frame wave functions. The parameters of the simplest Hulthen wave function have been chosen for the form factor $G(S)$, producing the correct nonrelativistic behavior in the two-nucleon rest-frame system.

Spin and isospin variables are neglected in our simple model. For such diagrams the isospin neglect does not lead to the loss of the diagram cancellation effects analogous to QCD [27]. The account of spin variables in the case of the nucleus breakup (Fig. 1) does not result in any diagram cancellations too.

The characteristic transverse momenta in the considered model of bremsstrahlung of scalar pions are about μ. In real multipion production the average transverse pion momentum $\langle p_t\rangle$ equals approximately 3μ. The calculations with the large $\langle p_t\rangle$ should lead to the increase of the observable coherent effects in the momentum spectra but the absolute cross section of this effect should be somewhat smaller (see the discussion in Sec. V).

The invariant amplitudes of the nucleon-nucleon elastic scattering M_1 and M_2 with propagators of nucleons give amplitudes of a pion emission. The imaginary NN amplitude with the slope parameter $b=1/(0.3\ \mathrm{GeV}/c)^2$ for the transverse momentum dependence is used. The amplitude as a sum of two time-ordered graphs, Fig. 1(b), was symmetrized for the momenta $\mathbf{k}_1$ and $\mathbf{k}_2$ taking into account the pion identity.

The pion radiation from external nucleon lines of the diagrams in Fig. 1 is neglected in the model considered. It does not change significantly the characteristic pion momentum in the region of the momentum transferred in the nucleon-nucleon scattering of the order of $1/\sqrt{b}$. So this approximation is not a principle for the qualitative results obtained.

Only the pole of the intermediate state propagator with two nucleons and one meson is taken into account in the integral calculation due to its minimal virtuality compared with the other intermediate states. The significant feature of the amplitudes in Fig. 1(b) is that the imaginary part of this propagator dominates with a good accuracy in Eq. (1), i.e.,

$$\frac{1}{E+i\eta-H}\approx -i\pi\delta(E-H). \tag{2}$$

Being done only with the real part of the propagator the numerical calculation of Eq. (1) gives a small value of about some percent. To explain qualitatively its smallness we use the approximate expression for the integrand. The dependence of the deuteron wave function on the longitudinal momentum can be written as

$$\phi(p'_{1l})\approx\varphi\left(p'_{1l}-\frac{E_0}{2}\right),\quad \varphi(k_l)=\varphi(-k_l).$$

If $\mathbf{u}_1=\mathbf{p}'_1+\mathbf{q}'_1=\mathbf{p}_1+\mathbf{q}_1+\mathbf{k}_1$, then

$$\frac{\phi_p(p'_{1l})\phi_q(q'_{1l})}{E_1+i\eta-E(p'_1)-E(q'_1)}\approx\frac{F(v_{1l})}{E_1-E_0-2v_{1l}+i\eta},$$

where

$$F(v_{1l})=\varphi\left(v_{1l}+\frac{u_{1l}}{2}\right)\varphi\left(-v_{1l}+\frac{u_{1l}}{2}\right),$$

$$v_{1l}=p'_{1l}-\frac{E_0+u_{1l}}{2}.$$

If $f(x)$ is the Fourier transform of $F(k)$, then one can write the next relation

$$\int_{-\infty}^{\infty}dk\frac{F(k)}{k-k_0-i\eta}=i\pi F(k_0)-2\pi\int_0^{\infty}dx f(x)\sin(k_0x).$$

The longitudinal momentum integration in Eq. (1) has the analogous form with $k_0=\Delta E=\frac{1}{2}(E_1-E_0)$. It is seen that the scattering amplitude depends on the energy nonconservation ΔE. The imaginary part is a narrow function with the maximum at $\Delta E=0$. The real part of the amplitude is equal to zero at this point and is small at large $|\Delta E|$ due to the integrand oscillation. This is the reason why the real part of the intermediate state propagator gives a small contribution in the scattering amplitude, Eq. (1).

For the collision of heavy nuclei we consider the nucleus in the single-particle approximation in which the nucleus wave function can be written as a product of single-particle ones:

$$\Phi(\mathbf{p}_1,\ldots,\mathbf{p}_N)=\prod_{i=1}^{N}\phi(p_i^*).$$

Here p^* is the nucleon momentum in the rest frame of the nucleon and the residue nucleus. In this model nucleons are treated as a gas of noninteracting particles and the characteristic space range is the nucleus radius. In the real model taking into account the interaction of nucleons this parameter could be some smaller. Nevertheless, the approximation used gives the correct qualitative behavior of studying coherent effects.

The single-particle wave function could be taken as the Fourier transform of a square root of the the nuclear density. For the gold nucleus this function is shown in Fig. 2 for a Fermi distribution with the radius $R=6.3$ fm and the diffuse parameter $a=1.0$ fm (the solid line), $a=0.6$ fm (the dashed line), and $a=0$ (the dotted line). For the last case it has the simple analytical form

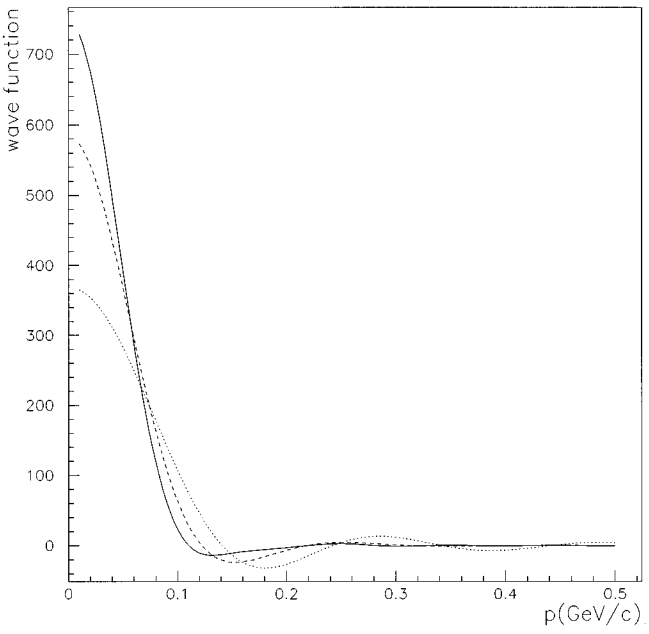

FIG. 2. The wave function for the nucleus with radius $R=6.3$ fm and diffuse parameter $a=1.0$ fm (the solid line), $a=0.6$ fm (the dashed line), and $a=0$ (the dotted line).

$$\phi(p)=\sqrt{\frac{12\pi}{R}}\frac{1}{p^2}\left(\frac{\sin(pR)}{pR}-\cos(pR)\right).$$

It is seen that the first zero point is at $pR\approx\frac{3}{2}\pi$. The numerical calculations were carried out with the value $a=1.0$ fm because calculations with the more realistic strongly oscillating wave function with $a=0.6$ fm require a lot of computer time. This approximation does not change the qualitative results obtained.

In the case of N interacting nucleon pairs the scattering amplitude has the next view

$$M=\prod_{i=1}^{N-1}\int\frac{d^3p'_i}{(2\pi)^3}\frac{\phi(p_i^*)\phi(q_i^*)}{2E(p'_i)2E(q'_i)}(-i\pi)\delta(E_i-E(p'_i)-E(q'_i))\frac{M_i}{h_i^2-m^2}\frac{\phi(p_N^*)\phi(q_N^*)}{2E(p'_N)2E(q'_N)}\frac{M_N}{h_N^2-m^2}. \tag{3}$$

For large N it approximates to the product of one-loop amplitudes analogous to the deuteron case.

The neglect of the real part of the intermediate state propagator simplifies the calculations considerably, retaining only the transverse momentum integration in Eqs. (1) and (3). The calculation of the cross section has to be done after that:

$$d\sigma\sim\int\prod_i d^3p_i d^3q_i d^3k_i(2\pi)^4\delta^{(4)}(P_f-P_i)|T|^2, \tag{4}$$

$$T=\frac{M}{2E_0\prod_i \sqrt{2E(p_i)2E(q_i)2\omega(k_i)}}.$$

III. QUANTUM MECHANICAL MONTE CARLO CALCULATION

Because of a large number both of internal variables of the integration in Eqs. (1), (3), and (4) and external ones it is natural to perform this integration in the Monte Carlo (MC) manner. We will name it here the quantum mechanical Monte Carlo calculation (QMMC) distinguishing it from conventional MC calculations. The coherent effects could not be included in the usual MC calculation as this approach is based on the probability of processes. The QMMC calculation is the usual MC method of manifold integration. It can be written as

$$\int_a^b dx f(x)\approx\frac{b-a}{N}\sum_{i=1}^{N} f(x_i). \tag{5}$$

In Eq. (5) we mean an integral of arbitrary dimension. This expression has the sense of a sum of weighted simulated events and allows one to obtain distributions of the arbitrary variable as the usual MC simulation:

$$\frac{dP}{dx}=f(x)\approx\frac{b-a}{N}\frac{1}{\Delta x}\sum_{\{\Delta x\}} f(x_i). \tag{6}$$

The real situation in Eq. (4) is complicated because of the inner one-loop integration in the amplitude. This case could be reduced to the QMMC procedure as

$$\int dx\left|\int dx_1 f(x,x_1)\right|^2=\int dx dx_1 dx_2 f(x,x_1)f^*(x,x_2)$$

$$\sim\frac{1}{N}\sum_{i,j,k} f(x_i,x_{1j})f^*(x_i,x_{2k}). \tag{7}$$

So it is possible to perform both internal and external integrations in a general manner, increasing the integral dimension.

Such a method of integration is successful only if the integration region has constant boundaries. In the opposite case [for example, in Eq. (1) with the real part of the propagator for an examination of Eq. (2)] the calculation of the internal integral with variable boundaries has to be done by lattice integration.

To avoid the narrow behavior of the integrand p_l and p_t^2 variables were substituted by those with a flat dependence of the integrand:

$$\int dx f(x)=\int dG(x)\frac{f(x)}{g(x)}.$$

The smoothing function $g(x)$ was chosen to be

$$g(p_l)=\frac{\alpha^2}{(p_l-p_{l0})^2+\alpha^2},$$

$$\alpha=\alpha_1,\quad p_l<p_{l0},\quad \alpha=\alpha_2,\quad p_l>p_{l0},$$

$$g(p_t^2)=\frac{\alpha^2}{p_t^2+\alpha^2}.$$

The parameter α was fitted from the view of different p_l, p_t^2 distributions in Eqs. (1), (3), and (4) for both internal and external variables.

IV. RESULTS FOR THE DEUTERON-DEUTERON SAMPLE

The results of the particle spectra calculation for the deuteron-deuteron case are shown in Figs. 3 and 4. At first we examine nucleon spectra to observe some general characteristics of collisions. There are two types of nucleons in this process: nucleons pion sources from the top jet in Fig. 1(b) moving to the right and accompanying nucleons from the bottom jet moving to the left. The distributions of the nucleon longitudinal momentum (left) and the transverse momentum square (right) are shown in Fig. 3. These spectra allow one to check at once the correspondence of the results to some qualitative features of the conventional pion emission in the nucleus-nucleus scattering.

There are spectra for accompanying nucleons in the upper row and that for the nucleons pion sources in the lower one. It is seen that the model describes correctly the main qualitative features of the process. The average momentum of accompanying nucleons is $\langle q_l\rangle=100$ GeV/c and the width of the distribution $\delta q_l\sim(p_F/m)p$ corresponds to the deuteron properties. Here $p_F\simeq 0.1$ GeV/c denotes the characteristic deuteron Fermi momentum and p is the average nucleon momentum in the moving deuteron. The transverse momentum corresponds to the slope parameter of NN scattering. The analogous distribution on p_l for the nucleon source is deformed and the spectrum of p_t^2 is widened due to the pion emission. The light picture shows the result with pion coherence effects taken into account; in the dark one, these effects are neglected.

The main questions connected with pion coherence can be understood from single-inclusive pion distributions. They are shown in Figs. 4(a) and 4(b) for the longitudinal momentum k_l and the square of the transverse momentum k_t^2. The distribution of k_l has the narrow maximum at $k_l\approx(\mu/m)p$, and μ is the pion mass. It corresponds to the pion bremsstrahlung mechanism and such an estimation could be obtained from the propagator consideration of the pion creation amplitude. The k_t^2 distribution has a narrow behavior with width $\delta k_t^2\approx\mu^2$. It is connected also with the pion radiation mechanism used.

The pion pseudorapidity distribution is shown in Fig. 4(c). The spectrum maximum at $\eta\approx 5.4$ corresponds to the maximum in the k_l distribution [Fig. 4(a)] and the angles are $\theta\approx m/p$ as in the conventional bremsstrahlung. The model considered is seen to give just large values of pion rapidities.

The spectra in Figs. 4(a) and 4(b) show that pion coherence increases the cross section in the maximum for about 20% both for the longitudinal and for the transverse momenta. Such a large interference appears to be not a trivial effect for a weakly bound deuteron, taking into account large values of the pion momenta. The reason lies in the large nucleon momentum spread in the rapidly moving deuteron

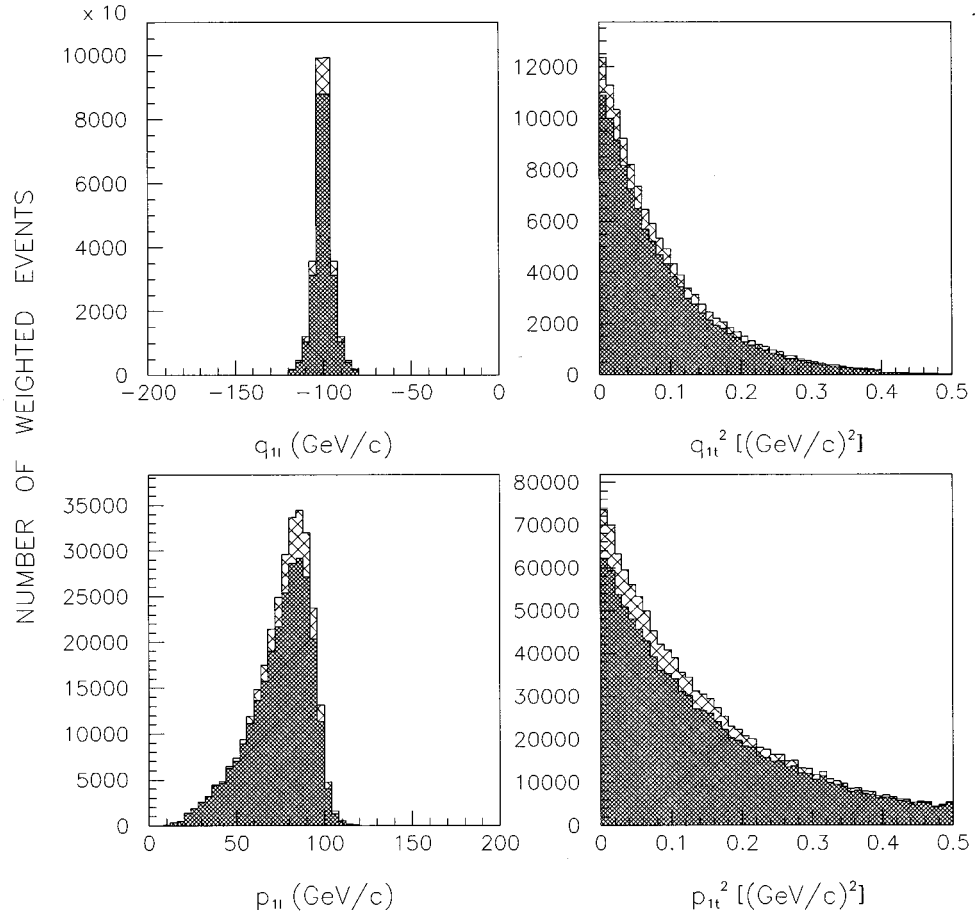

FIG. 3. The distributions of the nucleon longitudinal momentum (left) and the transverse momentum square (right). Spectra for the nucleon from the lower jet in Fig. 1(b) are in the upper row and those for the nucleon pion source are in the lower one. In the light histograms, the pion coherence is taken into account; the dark ones, the noncoherent contribution.

(see the q_l distribution in Fig. 3). It corresponds to the Lorentz shortening of the deuteron longitudinal scale $l=(m/p)l_0$ $(l_0\sim 1/p_F)$.

The pion coherence produces some narrowing of the k_t^2 distribution [Fig. 4(b)]. To see it better we examine the difference between light and dark spectra. It is just the interference contribution in the cross section connected with a pion identity. In Sec. VI interference terms will be shown to dominate in the cross section in the case of heavy nuclei due to the strong coherent enhancement with a large number of pion sources. So we estimate the situation with the large coherence by that spectra difference. It is shown in Figs. 4(d)–4(f) by dark histograms together with the noncoherent contribution (light spectra) normalized in the maximum. It is seen that the coherence narrows both the longitudinal and the transverse momentum distributions. The longitudinal momentum spectrum is narrowed around the characteristic value $\sim(\mu/m)p$. It is not softened by coherence. The narrowing of the transverse momentum spectrum has been already discussed in the literature [28].

As a consequence of the coherent effects obtained for the pion momentum spectra the pseudorapidity distribution for the coherent contribution is shifted to the right relative to the noncoherent one [Fig. 4(f)].This effect is rather small in the deuteron-deuteron sample; however, it increases for heavy nuclei.

V. THE HEAVY NUCLEI SAMPLE

In the case of gold-gold collisions two and three interacting nucleon pairs are considered [Fig. 1(a)]. Only one pion is created in every nucleon-nucleon interaction. The residual nuclei are introduced in the model, Fig. 1(a), to provide the energy-momentum conservation in Eq. (4). In the first variant the coherent increase of the cross section in the maximum of the transverse momentum spectra is approximately 3.8%. Such a decrease of the coherent enhancement in comparison with the deuteron case is a consequence of a decrease of the momentum space coherence volume due to the nucleus radius growth. Pion spectra for the coherent contribution together with the noncoherent spectra are shown in Figs. 5(a)–5(c). All qualitative results for the deuteron-deuteron case are confirmed here. The difference is that the narrowing of longitudinal and transverse momentum spectra is stronger in this case. As a consequence the shift of the pseudorapidity distribution to the right is rather large. It is about one unit in the rapidity scale. Such an increase of the effect is due to the large nucleus radius also as the characteristic width of the longitudinal and transverse momentum

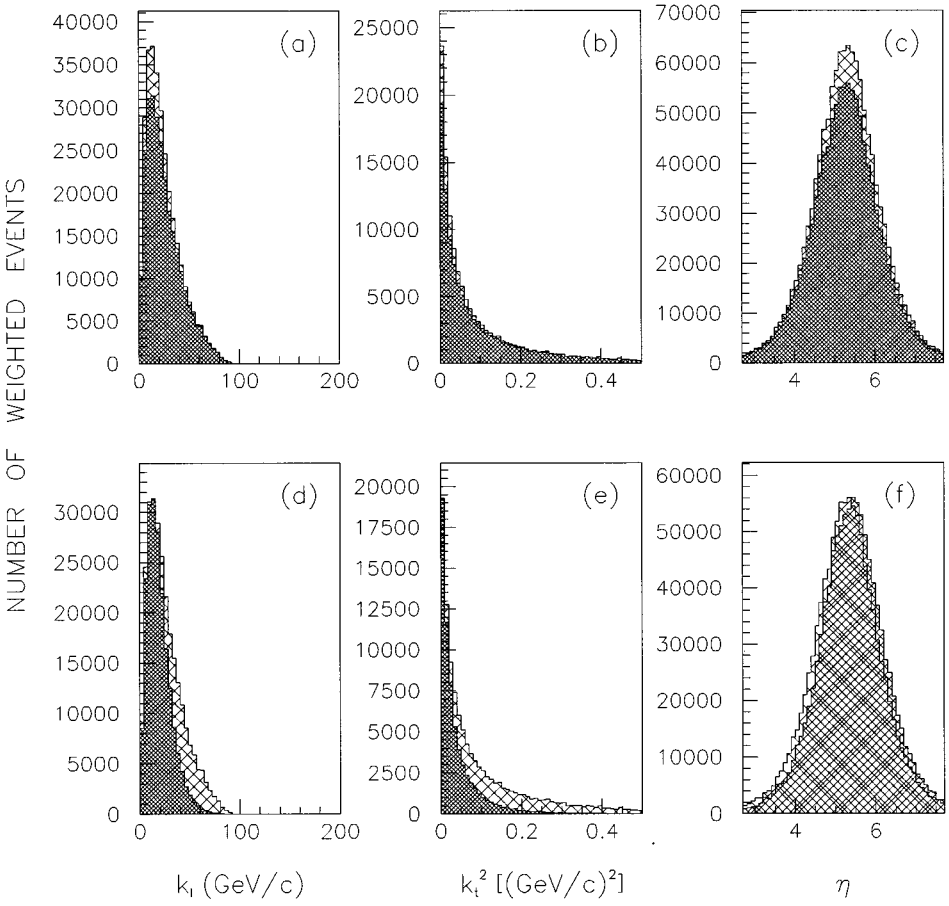

FIG. 4. The distributions of the pion longitudinal momentum (a),(d), the transverse momentum square (b),(e), and the pion pseudorapidity distribution (c),(f). In the light histograms in (a)–(c), the pion coherence is taken into account; the dark ones, the noncoherent contribution. In the dark histograms in (d)–(f), the interference part; the light one, the noncoherent contribution.

distributions for the coherent pion radiation is of an order of the inverse space range.

In the second variant with three interacting nucleon pairs the absolute value of the coherent cross-section increase is approximately 7.8% in the maximum of the transverse momentum spectrum. It corresponds to the estimation on this value given in Sec. VI which is roughly twice as large as that in the first variant. The pion momentum spectra correspond approximately to the two-pion case.

The model examined for pion creation in nucleus-nucleus collisions yields pions at random over the whole nucleus in the correspondence with the wave functions in Eq. (3). In reality there is some correlation of the pion radiation and some retarding effects due to the Glauber screening of nucleons in the scattering process. One can calculate it in some effective manner in the framework of the QMMC approach. The nucleus-nucleus collision can be treated as a sequence of collisions of the corresponding layers of the nuclei. The layer thickness 2σ is a free path length of a nucleon. The single-particle nucleus wave function can be represented as the superposition of layer wave functions treated as a product of longitudinal and transverse coordinate wave functions:

$$\psi(\mathbf{r})=\sum_{k=-M}^{M}\psi_{1k}(z)\psi_{2k}(\mathbf{b}). \tag{8}$$

The function $\psi_{1k}(z)$ is a square root of the Gauss distribution with the dispersion σ centered at z_k. The second function $\psi_{2k}(\mathbf{b})$ depending on the impact parameter b is a square root of the Fermi distribution with radius R_k. The Fourier transform of it is the product of the longitudinal momentum function

$$\phi_1(p_l)=e^{-ip_lz_k}g(p_l)$$

and the transverse momentum one

$$\phi_2(p_t,R_k)=2\pi\int_0^\infty bdb\,\psi_{2k}(b)J_0(p_tb).$$

The function $g(p_l)/\sqrt{2\pi}$ is a square root of the Gauss distribution with the dispersion $(2\sigma)^{-1}$.

To take into account the Glauber screening one can substitute the Fourier transform of the wave function, Eq. (8), into Eq. (3) with only the correspondent layers in the sum, Eq. (8), remaining. As a result the next substitution has to be done in Eq. (3):

$$\phi(p_i^*)\phi(q_i^*)\rightarrow\phi_0(p_i^*)\phi_0(q_i^*)+2\sum_{k=1}^{M}\cos[(p_{il}^*-q_{il}^*)z_k]$$
$$\times\phi_k(p_i^*)\phi_k(q_i^*), \tag{9}$$

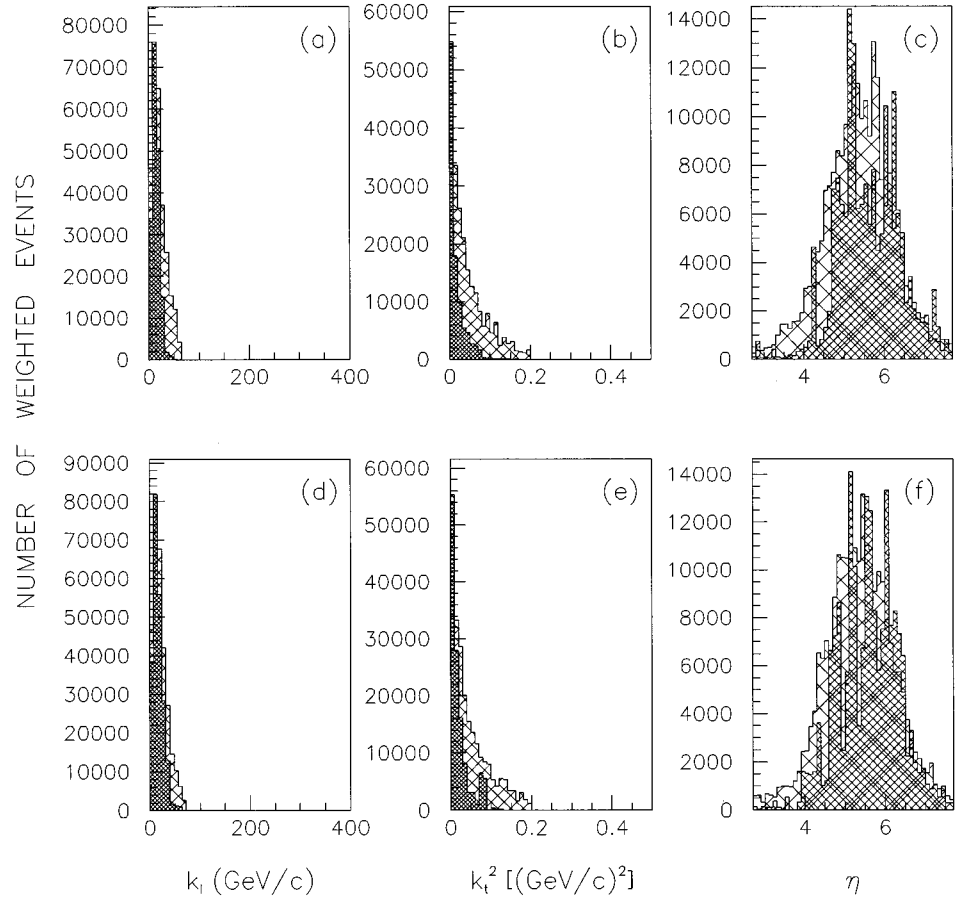

FIG. 5. The distributions of the pion longitudinal momentum (a),(d), the transverse momentum square (b),(e), and the pion pseudorapidity distribution (c),(f). In the dark histograms, the interference contribution; the light one, the noncoherent part. In (d)–(f) the Glauber screening is taken into account.

$$\phi_k(p^*)=g(p_l^*)\phi_2(p_t,R_k).$$

The nuclear density as a function of z was fitted in the calculation by a square of the sum of 11 Gauss distributions ($M=5$). The distance between the layers is 2.3σ ($\sigma=0.5$ fm).

The results of the calculation are shown in Figs. 5(d)–5(f). The Glauber screening is seen to lead to some decrease of the coherent narrowing of the longitudinal momentum distribution. The reason for it is an increase of the characteristic longitudinal momentum of a nucleon in the integral, Eq. (3). In the first case it is of an order of the inverse nucleus range due to $\phi(p_i^*)$. After the Glauber correction is done it is determined by the free path length 2σ in the function $g(p_l)$ and by an oscillation factor in Eq. (9) with the momentum differences being significant there. It enhances the large longitudinal momenta in the integral compared with the first case. The transverse momentum distribution and its narrowing are not influenced by Glauber screening. The coherent shift of the pseudorapidity spectrum to the right is smaller [Fig. 5(f)] than that in Fig. 5(c). Nevertheless, it is about one-half of a unit in the rapidity scale and seems to be observable in the experiment.

VI. COHERENT ENHANCEMENT WITH A LARGE NUMBER OF PION SOURCES

The real situation of central nucleus-nucleus collisions with a large number of pion sources $\sim 10^2$ could not be studied in the QMMC manner because of the enormous number of permutations. To calculate physical effects in this case it is necessary to do some additional approximations starting from the results obtained. The symmetrized amplitude Fig. 1(a) can be written as

$$T=\sum_i t(k_{i1},v_1;\ldots;k_{iN},v_N),\quad v_j=\{p_j,q_j\},$$

the summing being done over all pion permutations. For a large number of interacting nucleon pairs, N, the amplitude, Eq. (3), is seen to be a product of the effective nucleon-nucleon amplitudes of pion creation:

$$t(k_{i1},v_1;\ldots;k_{iN},v_N)\approx\prod_{n=1}^{N}\tau(k_{in},v_n). \tag{10}$$

One can perform an integration on the nucleon variables v in Eq. (4) by introducing the correlation function $G(k_i,k_j)$:

$$G(k_i,k_j)=\int dv\,\tau(k_i,v)\,\tau^*(k_j,v)$$
$$=\sqrt{\frac{dW_0}{dk_i}}\sqrt{\frac{dW_0}{dk_j}}g(k_i-k_j), \qquad (11)$$

where dW_0/dk_i is the single-inclusive pion distribution in the nucleon-nucleon scattering. The function $g(k_i-k_j)$ can be approximated by a Gauss distribution with the dispersion γ obtained in the QMMC calculation and is normalized as $g(0)=1$.

Because of the factorization property of the amplitude, Eq. (10), the differential cross section has the next form

$$\frac{dW}{dk_1\cdots dk_N}=\prod_{n=1}^{N}\int dv_n\sum_{i,j}\tau(k_{in},v_n)\,\tau^*(k_{jn},v_n).$$

Using Eq. (11) the integration on nucleon variables can be performed. The pion momenta distribution can be decomposed into the noncoherent part and the interference one,

$$\frac{dW}{dk_1\cdots dk_N}=N!\frac{dW_0}{dk_1}\cdots\frac{dW_0}{dk_N}+N!\sum_{i=2}^{N!}D_i, \qquad (12)$$

$$D_i=G(k_1,k_{i1})\cdots G(k_N,k_{iN})=\prod_{m=1}^{M_i}R_m^l,$$

where R_m^l denotes the cycle of the length l:

$$R_m^l=G(k_{m1},k_{m2})G(k_{m2},k_{m3})\cdots G(k_{ml},k_{m1}).$$

There are M_i cycles for every ith permutation in the sum, Eq. (12).

To do the integration on pion momenta in Eq. (12) for a single-inclusive pion distribution to be obtained it is convenient to treat dW_0/dk_i in the Gauss form with the average value k_0 and the dispersion γ_0. As a result the next expression is deduced for such a distribution after the straightforward but rather long calculations (see the Appendix):

$$(N-1)!\frac{dW}{dk_1}=N!\frac{dW_0}{dk_1}+N!\sum_{i=2}^{N!}B(l_1)\exp\left(-\frac{(k_1-k_0)^2}{2S_{l_1-1}^2}\right)$$
$$\times\prod_{m=2}^{M_i}B(l_m)(2\pi S_{l_m-1}^2)^{3/2}. \qquad (13)$$

The different values in Eq. (13) are given by the following formulas through Gauss-distribution parameters:

$$\sigma_p^2=\gamma^2+\frac{\gamma_0^2\sigma_{p-1}^2}{\gamma_0^2+\sigma_{p-1}^2},$$

$$P_l=\prod_{p=1}^{l}\frac{\gamma_0^2}{\gamma_0^2+\sigma_{p-1}^2},$$

$$\frac{1}{S_{l-1}^2}=\sum_{p=1}^{l-1}\frac{1}{\gamma_0^2+\sigma_{p-1}^2}P_{p-1}^2+\frac{1}{\gamma_0^2}+\frac{(1-P_{l-1})^2}{\sigma_{l-1}^2},$$

$$B(l)=\left(\frac{1}{2\pi\gamma_0^2}\right)^{3/2l}\prod_{p=1}^{l-1}\left(\frac{2\pi}{(1/\gamma_0^2)+(1/\gamma^2)+(1/\sigma_{p-1}^2)}\right)^{3/2}. \qquad (14)$$

The value σ_p is expressed through the recurrent relation in Eq. (14) with $\sigma_0=\gamma$ and $P_0=1$. The quantities $S_{l-1}=\gamma_0$ and $B(l)=(2\pi\gamma_0^2)^{-3/2}$ have to be taken when $l=1$.

One can change the summing up on permutations in Eq. (13) to that on the cycles lengths $l_1,l_2,\ldots,l_M$ $(l_1+l_2+\cdots+l_M=N)$. It can be done due to the fact that the expression under the sum sign in Eq. (13) depends only on these values [see Eq. (A6) in the Appendix):

$$\sum_{i=2}^{N!}\{\cdots\}\rightarrow{\sum_{l_1l_2\cdots l_M}}'A_{l_1-1}^{N-1}$$
$$A_{l_2-1}^{N-l_1-1}\cdots A_{l_M-1}^{N-l_1-l_2-\cdots-l_{M-1}-1}\{\cdots\},$$

$$A_m^n=n!/(n-m)!. \qquad (15)$$

It is necessary to exclude the term with $l_1=l_2=\cdots=l_M=1$ from the summing up.

A simpler formula in comparison with Eq. (13) can be obtained in the case of a narrow correlation function $\gamma^2\ll\gamma_0^2$ and for a small number of pion sources N when $\sigma_{p-1}^2\ll\gamma_0^2$ in Eq. (14):

$$(N-1)!\frac{dW}{dk_1}=N!\frac{dW_0}{dk_1}+N!\sum_{i=2}^{N!}\left(\frac{dW_0}{dk_1}\right)^{l_1}$$
$$\times(2\pi\gamma^2)^{3(l_1-1)/2}\left(\frac{1}{l_1}\right)^{3/2}$$
$$\times\prod_{m=2}^{M_i}\left(\frac{\gamma}{\gamma_0}\right)^{3(l_m-1)}\left(\frac{1}{l_m}\right)^3. \qquad (16)$$

Then for the collision with two- and three-pion sources the distribution in the maximum point has the next values, for $N=2$,

$$\frac{dW}{dk_1}(k_0)=2\frac{dW_0}{dk_1}(k_0)\left[1+\left(\frac{1}{\sqrt{2}}\right)^3\epsilon\right]$$

and, for $N=3$,

$$2!\frac{dW}{dk_1}(k_0)=6\frac{dW_0}{dk_1}(k_0)\left[1+\frac{1}{8}\epsilon+2\left(\frac{1}{\sqrt{2}}\right)^3\epsilon\right]. \qquad (17)$$

The value $\epsilon=(\gamma/\gamma_0)^3$ is the probability for two pions to be in the coherent range $\sim\gamma^{-1}$, i.e., to be in the same state. As noted in Sec. V, Eq. (17) shows that the coherent enhancement in the maximum point is roughly twice as large in the three-pion case as that in the two-pion case.

It is possible now to illustrate the validity of the assumption made in Sec. IV that the interference contribution in the cross section of the two-pion sample gives a reliable estima-

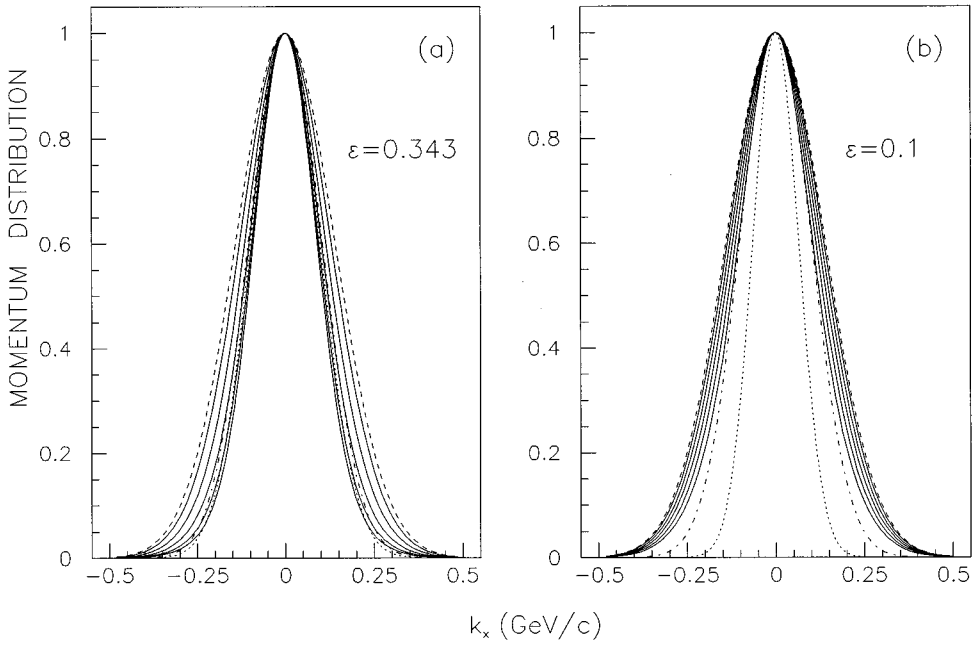

FIG. 6. The single-inclusive pion momentum distribution with $N=4$, 8, 12, and 20 interacting nucleon-nucleon pairs (solid lines) for two values of the ϵ parameter. The dot-dashed line, the coherent contribution in the two-pion case. The dashed line, the noncoherent contribution, and the dotted line shows the correlation function.

tion for the real many-pion case. One can be convinced using formulas (13)–(15) for the arbitrary component of the pion momentum. To obtain the large coherent effects already at low N the rather large value $\gamma=0.7\gamma_0$ ($\gamma_0=\mu$) was chosen for the dispersion of the correlation function. The result for the single-inclusive pion distribution is offered in Fig. 6(a) by solid lines for different variants with N equal to 4, 8, 12, 16, and 20. The coherent contribution for the two-pion sample is shown by the dot-dashed line, the noncoherent cross section being presented by the dashed one. All curves are normalized in the maximum. The different variants are seen to converge to some limit curve with the growth of N coinciding approximately with the correlation function (dotted line). This curve is close to the dot-dashed one. So such interference terms actually dominate in this case in the single-inclusive pion cross section at large N and the two-pion variant gives a reliable estimate of the coherent narrowing of the momentum spectrum. The measure of the inaccuracy in such an estimation could be the distinction of this distribution from the correlation function.

The QMMC calculation in Sec. V gives for the ϵ parameter $\epsilon\approx 0.1$ by means of Eq. (17) from the coherent enhancement in the cross section. The formulas (13)–(15) with the corresponding γ show that the coherent contribution for the two-pion sample gives a conservative estimate of the spectra narrowing in this case [Fig. 6(b)]. The real coherent effects are somewhat stronger. Nevertheless, such interference terms give a significant contribution in the cross section and give the correct qualitative estimate of the coherent narrowing of momentum distributions. The additional increase of the transverse momentum spectrum narrowing has to be due to the growth of the characteristic $\langle p_t\rangle$ in the noncoherent distribution to the quantity $\langle p_t\rangle\approx 3\mu$ in correspondence with the experimental value. The coherent effect in the pseudorapidity spectra will be stronger too.

One can calculate the coherent enhancement in the maximum of the momentum distribution using Eqs. (13)–(15). The behavior of the ratio of the interference contribution to the noncoherent one as a function of the number of interacting nucleon pairs, N, is shown in Fig. 7 with different quantities of the parameter ϵ. It is seen that this function has the threshold character, demonstrating very strong growth with the increasing of N. To understand qualitatively such a behavior it is useful to consider the structure of the simplified

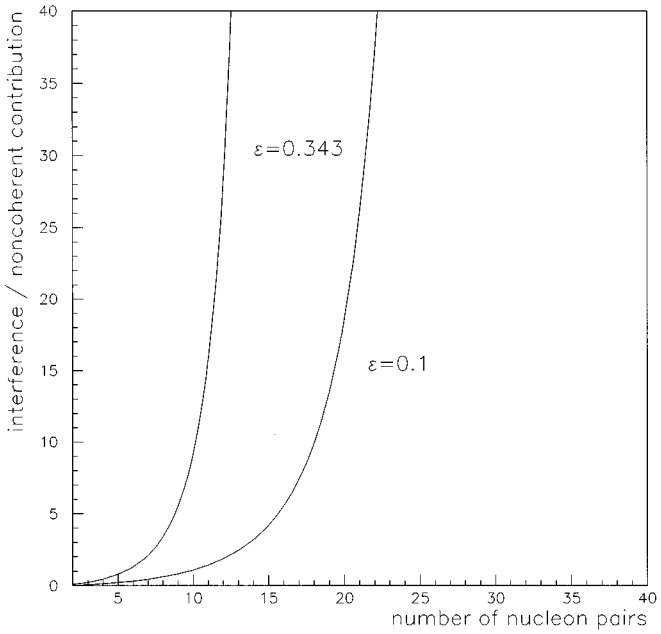

FIG. 7. The coherent enhancement as a function of the number of interacting nucleon pairs N for two values of the ϵ parameter.

formula Eq. (16). Every term in the sum is proportional to some degree of ϵ and the number of terms is $(N!)^2$. It is convenient to introduce the parameter $A=\epsilon^{N-1}N!$ [5] as a measure of the coherent enhancement reproduced by Eq. (13). It has a transparent physical sense. The first factor with the degree of ϵ is the depressing factor connected with the small probability for N pions to be in the same state. The second factor is the usual laser-type enhancement due to the coherent induced radiation [4,5]. The drastic character of the threshold function is connected with the strong competition of depressing and enhancing factors in A at large N.

It is seen in Fig. 7 that the threshold value of N is of the order of 20's in the case $\epsilon=0.1$. Taking into account the increase of the characteristic $\langle p_t\rangle$ for the pion bremsstrahlung from μ to 3μ one can estimate this threshold to be about 10^2. In a real situation with the pion multiplicity in the nucleon-nucleon interaction of the order of tens the threshold is clear to be decreased again and coherent effects considered in Sec. V could be observable in experiments. The pion multiplicity can be used here as an enhancing factor for the coherent effects both in inclusive and event-by-event approaches. The quantitative consideration with the real pion multiplicity in the nucleon-nucleon interaction could give reliable values of the effects discussed.

The strong coherent enhancement in Fig. 7 seems to be unphysical when the pion radiation cross section became larger than the geometrical one for the central nucleus-nucleus collision. The cut of the growth could be done by diagrams with the additional pions created in the intermediate state and absorbed by an external prong. The amplitudes of pion creation and absorption have an opposite sign due to the pion-nucleon propagator. So there is the destructive interference of the imaginary part of such diagrams and amplitudes, Fig. 1(a).

The probability ϵ for two pions to be in the same state depends on the inverse slope parameter $\gamma_0\sim\langle p_t\rangle$ of the p_t distribution. From a number of different mechanisms of elementary pion creation the most important one in central nucleus-nucleus collisions could be the mechanism with the smallest γ_0 due to coherence.

VII. CONCLUSIONS

The consideration of coherent effects in nucleus-nucleus scattering by virtue of quantum mechanical Monte Carlo calculations allows one to come to the following conclusions.

(1) The model of bremsstrahlung of scalar pions shows that pions at large rapidities can be radiated with a strong coherence.

(2) The coherent enhancement has the threshold character as a function of the number of interacting nucleon pairs.

(3) The coherence narrows regions of pion transverse momenta towards zero and longitudinal momenta around some characteristic value.

(4) The pion pseudorapidities are moved towards the large values of about one-half of a unit.

In the model examined the pion bremsstrahlung mechanism gives one pion with a large rapidity. In real multiperipheral pion radiation the effects obtained could take place for pions from every step of the ladder. As a result the narrowing of the $\langle p_t\rangle$ distribution and the shift of the pseudorapidity spectrum to the right could take place in this case too. To search experimentally for the discussed coherent effects, it is reasonable to compare pseudorapidity distributions in proton-proton interactions with those for central nucleus-nucleus collisions. The region from the shoulder in the plateau $\eta\approx 2.5$ to the end of the spectrum is relevant. One can try to observe the threshold character of effects using pion multiplicity and the number of baryons at small angles as a measure of the impact parameter.

It is naturally to combine the search of isospin fluctuations with the coherent effects discussed. The experimental observation could be realized in both inclusive and in event-by-event approaches.

ACKNOWLEDGMENTS

I would like to express my gratitude to A.A. Anselm and M.G. Ryskin for interesting and fruitful discussions during the entire period of the work. I am grateful to J.W. Harris, T. Hallman, and L.S. Schroeder for the hospitality at LBL where this work was discussed. I would like to thank X.N. Wang and the staff of the theory division of LBL for very interesting seminar on this work. I thank M.N. Strikhanov for help in executing this work.

APPENDIX: DETAILS OF THE COHERENT ENHANCEMENT CALCULATION

To obtain a single-inclusive pion distribution it is necessary to integrate Eq. (12) on $N-1$ pion momenta. The first integration of the Gauss functions gives the next result

$$\int d\mathbf{k} g_{\gamma_1}(\mathbf{k}_1-\mathbf{k})\frac{dW_0}{dk}g_{\gamma_2}(\mathbf{k}-\mathbf{k}_2)$$
$$=g_{\sigma_1}(\mathbf{k}_1-\mathbf{k}_2^1)\left(\frac{1}{2\pi\gamma_0^2}\right)^{3/2}\left(\frac{2\pi}{(1/\gamma_1^2)+(1/\gamma_0^2)+(1/\gamma_2^2)}\right)^{3/2}$$
$$\times\exp\left(-\frac{(\mathbf{k}_2-\mathbf{k}_0)^2}{2(\gamma_0^2+\gamma_2^2)}\right),$$

with

$$\sigma_1^2=\gamma_1^2+\frac{\gamma_0^2\gamma_2^2}{\gamma_0^2+\gamma_2^2},\quad \mathbf{k}_2^1=\frac{(\mathbf{k}_2/\gamma_2^2)+(\mathbf{k}_0/\gamma_0^2)}{(1/\gamma_0^2)+(1/\gamma_2^2)}.$$

Then the circle integration can be performed:

$$\int d\mathbf{k_1}\cdots d\mathbf{k_p}\frac{dW_0}{dk_1}g(\mathbf{k}_1-\mathbf{k}_2)\cdots\frac{dW_0}{dk_p}g(\mathbf{k}_p-\mathbf{k}_1)$$
$$=A_1\cdots A_{p-1}\left(\frac{1}{2\pi\gamma_0^2}\right)^{3(p-1)/2}$$
$$\times\int d\mathbf{k}_1 g_{\sigma_{p-1}}(\mathbf{k}_1-\mathbf{k}_1^{p-1})\frac{dW_0}{dk_1}$$
$$\times\exp\left(-\frac{(\mathbf{k}_1^{p-2}-\mathbf{k}_0)^2}{2(\gamma_0^2+\sigma_{p-2}^2)}\right)\cdots\exp\left(-\frac{(\mathbf{k}_1^1-\mathbf{k}_0)^2}{2(\gamma_0^2+\sigma_1^2)}\right)$$
$$\times\exp\left(-\frac{(\mathbf{k}_1-\mathbf{k}_0)^2}{2(\gamma_0^2+\gamma^2)}\right),\qquad\text{(A1)}$$

where

$$\sigma_p^2=\gamma^2+\frac{\gamma_0^2\sigma_{p-1}^2}{\gamma_0^2+\sigma_{p-1}^2},\quad \mathbf{k}_1^p=\frac{(\mathbf{k}_1^{p-1}/\sigma_{p-1}^2)+(\mathbf{k}_0/\gamma_0^2)}{(1/\sigma_{p-1}^2)+(1/\gamma_0^2)},$$
$$\sigma_0^2=\gamma^2,\quad \mathbf{k}_1^0=\mathbf{k}_1, \tag{A2}$$

and

$$A_p=\left(\frac{2\pi}{(1/\gamma_0^2)+(1/\gamma^2)+(1/\sigma_{p-1}^2)}\right)^{3/2}.$$

Using Eq. (A1) we obtain for the single-inclusive pion distribution the formula

$$(N-1)!\frac{dW}{dk_1}=N!\frac{dW_0}{dk_1}+N!\sum_{i=2}^{N!}\left(\prod_{p=1}^{l_1-1}A_p\frac{dW_0^{p-1}}{dk_1}\right)\times\frac{dW_0}{dk_1}g^{l_1-1}(\mathbf{k}_1-\mathbf{k}_1^{l_1-1})\prod_{m=2}^{M_i}\times\int d\mathbf{k}\left(\prod_{p=1}^{l_m-1}A_p\frac{dW_0^{p-1}}{dk}\right)\frac{dW_0}{dk}\times g^{l_m-1}(\mathbf{k}-\mathbf{k}^{l_m-1}), \tag{A3}$$

with

$$\frac{dW_0^p}{dk_1}=\left(\frac{1}{2\pi\gamma_0^2}\right)^{3/2}\exp\left(-\frac{(\mathbf{k}_1^p-\mathbf{k}_0)^2}{2(\gamma_0^2+\sigma_p^2)}\right),$$
$$g^p(\mathbf{k})\equiv g_{\sigma_p}(\mathbf{k}),$$

and $g^0=1$.

On the base of the recurrent relation (A2) the momentum $\mathbf{k}^l$ is given by

$$\mathbf{k}^l=P_l(\mathbf{k}-\mathbf{k}_0)+\mathbf{k}_0,\quad P_l=\prod_{p=1}^{l}\frac{\gamma_0^2}{\gamma_0^2+\sigma_{p-1}^2}. \tag{A4}$$

Then the integral in Eq. (A3) can be calculated:

$$\int d\mathbf{k}\left(\prod_{p=1}^{l-1}A_p\frac{dW_0^{p-1}}{dk_1}\right)\frac{dW_0}{dk}g^{l-1}(\mathbf{k}-\mathbf{k}^{l-1})=\left(\prod_{p=1}^{l-1}A_p\right)\left(\frac{1}{2\pi\gamma_0^2}\right)^{3l/2}(2\pi S_{l-1}^2)^{3/2},$$

with

$$\frac{1}{S_{l-1}^2}=\sum_{p=1}^{l-1}\frac{1}{\gamma_0^2+\sigma_{p-1}^2}P_{p-1}^2+\frac{1}{\gamma_0^2}+\frac{(1-P_{l-1})^2}{\sigma_{l-1}^2}.$$

Finally, substituting this result into Eq. (A3) and using Eq. (A4) we obtain the single-inclusive pion momentum distribution

$$(N-1)!\frac{dW}{dk_1}=N!\frac{dW_0}{dk_1}+N!\sum_{i=2}^{N!}\left(\prod_{p=1}^{l_1-1}A_p\right)\left(\frac{1}{2\pi\gamma_0^2}\right)^{3l_1/2}\times\exp\left(-\frac{(k_1-k_0)^2}{2S_{l_1-1}^2}\right)\prod_{m=2}^{M_i}\left(\prod_{p=1}^{l_m-1}A_p\right)\times\left(\frac{1}{2\pi\gamma_0^2}\right)^{3l_m/2}(2\pi S_{l_m-1}^2)^{3/2}. \tag{A5}$$

Let us express the sum on permutations in Eq. (A5) through the sum on cycle lengths. It is necessary at first to consider permutations produced from the initial one and having a cycle of length l_1 beginning from the first element. The number of them is $A_{l_1-1}^{N-1}$, where $A_m^n=n!/(n-m)!$. After that one has to add analogous permutations with cycles of length l_2 among the remaining elements of the first permutation. The summary number of such permutations will be $A_{l_1-1}^{N-1}A_{l_2-1}^{N-l_1-1}$. The total amount of permutations with cycle lengths $l_1,l_2,\ldots,l_M$ $(l_1+l_2+\cdots+l_M=N)$ is $A_{l_1-1}^{N-1}A_{l_2-1}^{N-l_1-1}\cdots A_{l_M-1}^{N-l_1-l_2-\cdots-l_{M-1}-1}$ and we obtain the next formula for the sum in Eq. (A5):

$$\sum_{i=2}^{N!}\{\cdots\}\rightarrow{\sum_{l_1l_2\ldots l_M}}' A_{l_1-1}^{N-1}A_{l_2-1}^{N-l_1-1}\cdots A_{l_M-1}^{N-l_1-l_2-\cdots-l_{M-1}-1}\times\{\cdots\}. \tag{A6}$$

Here Σ' means that the term with $l_1=l_2=\cdots=l_M=1$ is excluded from the summing up.

[1] C.M.G. Lattes, Y. Fujimoto, and S. Hasegawa, Phys. Rep. **65**, 151 (1980).

[2] S. Hasegawa, in Proceedings of the Fifth International Symposium on Very High Energy Cosmic Ray Interactions, Tarbes 1990, edited by I.N. Capdevielle and P. Gabinski (unpublished), p. 227; J. Bartke, E. Gladysz-Dziadus, M. Kowalski, P. Stefanski, and A.D. Panagiotou, Report No. ALICE/93-12, 1993.

[3] I.V. Andreev, JETP Lett. **33**, 384 (1981).

[4] V. Karmanov and A. Kudrjavtsev, Report No. ITEP-88, 1983; in Proceedings of the Symposium on Nucleon-Nucleon and Hadron-Nucleus Interactions at Intermediate Energy, Lenin-

grad, 1986 (unpublished), p. 300.
[5] C. Lam and S. Lo, Phys. Rev. Lett. **52**, 1184 (1984); Phys. Rev. Lett. D **33**, 1336 (1986); Int. J. Mod. Phys. A **1**, 451 (1986); Phys. Rev. D **33**, 1336 (1986).
[6] A. A. Anselm, Phys. Lett. B **217**, 169 (1989); A.A. Anselm and M.G. Ryskin, Phys. Lett. B **266**, 482 (1991).
[7] J.P. Blaizot and A. Krzywicki, Phys. Rev. D **46**, 246 (1992).
[8] J.D. Bjorken, Acta Phys. Pol. B **23**, 637 (1992); Int. J. Mod. Phys. A **7**, 4189 (1992); Report No. SLAC-PUB-6488, 1994.
[9] A. Anselm and M. Bander, Report No. UCI-TR 93-32, 1993.
[10] C. Greiner, C. Gong, and B. Muller, Phys. Lett. B **316**, 226 (1993).
[11] Z. Huang, Report No. LBL-34703, 1993.
[12] Z. Huang and X.N. Wang, Report No. LBL-34931, 1993.
[13] S.Yu. Khlebnicov, Mod. Phys. Lett. A **8**, 190 (1993).
[14] I. Kogan, Phys. Rev. D **48**, 3971 (1993).
[15] S. Pratt, Phys. Lett. B **301**, 159 (1993).
[16] K. Rajagopal and F. Wilczek, Nucl. Phys. **B399**, 395 (1993); **B404**, 577 (1993).
[17] J.P. Blaizot and D. Diakonov, Phys. Lett. B **315**, 226 (1993).
[18] S. Pratt and W. Bauer, Phys. Lett. B **329**, 413 (1994).
[19] S. Gavin and B. Muller, Phys. Lett. B **329**, 486 (1994).
[20] S. Gavin, A. Gocksch, and R. Pisarski, Phys. Rev. Lett. **72**, 2143 (1994).
[21] G.F. Bertsch, Phys. Rev. Lett. **72**, 2349 (1994).
[22] Z. Huang, Phys. Rev. D **49**, 16 (1994).
[23] S. Pratt and V. Zelevinsky, Phys. Rev. Lett. **72**, 816 (1994).
[24] S. Pratt and W. Bauer, Phys. Lett. B **329**, 413 (1994).
[25] T.D. Cohen, M.K. Banerjee, M. Nielsen, and X. Jin, Phys. Lett. B **333**, 166 (1994).
[26] M. Gyulassy, S.K. Kauffmann, and Lance W. Wilson, Phys. Rev. C **20**, 2267 (1979).
[27] Yu.I. Dokshitzer, V.A. Khoze, S.I. Troyan, and A.H. Mueller, Rev. Mod. Phys. **60**, 373 (1988).
[28] I.N. Mishustin, L.M. Satarov, J. Maruhn, H. Stocker, and W. Greiner, Z. Phys. A **342**, 309 (1992).